Asian Journal of Chemistry; Vol. 26, No. 24 (2014), 8397-8401

ASIAN JOURNAL OF CHEMISTRY

http://dx.doi.org/10.14233/ajchem.2014.17647

Improvement Photocatalytic Activity of Ag_2S Nanoparticles by Gold Doping

E.S. BAEISSA

Chemistry Department, Faculty of Science, King Abdulaziz University, P.O. Box 80203 Jeddah 21589, Saudi Arabia

Corresponding author: Fax: +96 62 6952292; Tel: +96 62 6400000; E-mail: elhambaeissa@gmail.com

Received: 22 March 2014; *Accepted*: 2 April 2014; *Published online*: 1 December 2014; AJC-16369

Hydrothermal method was used to prepare Ag_2S nanoparticles, photoassisted deposition method was used to doped gold into Ag_2S nanoparticles. The obtained nanoparticles are characterized by X-ray photoelectron spectroscopy, photoluminescence emission spectra, ultraviolet and visible spectroscopy, surface area measurement, X-ray diffraction and transmission electron microscopy. The photocatalytic removal of cyanide under visible light was used to measure photocatalytic performance of Ag_2S and Au/ Ag_2S nanoparticles. The results reveal that doping of gold into Ag_2S cause shift absorption of Ag_2S to high wavelength as shown in UV-visible spectra. XPS results confirm the presence of gold metal above surface of Ag_2S nanoparticles. 0.6 wt % Au/Ag_2S nanoparticle has highest photocatalytic activity and is stable after reuse for five times.

Keywords: Au loading, Ag_2S, Visible photocatalyst, Oxidation of cyanide.

INTRODUCTION

Cyanide usually found in many inorganic and organic compounds. All forms of cyanide are toxic and posses risk hazard at elevated concentrations, but the most hazardous form is hydrogen cyanide. Exposure to cyanide causes neurological effects such as tremors and rapid breathing. If the exposure to cyanide was for long period of time, nerve damage, weight loss, thyroid effects and death could occur[1]. Cyanide is an inorganic pollutant which release in the aquatic environment from different anthropogenic sources. For example it produced from the use of cyanide-containing road salts iron from different industries such as photography, pharmaceuticals, plastics, ore leaching, metal mining, finishing, cleaning, plating, processing, electroplating, automobile parts manufacture, steel mills, steel tempering and coal coking[2,3] cyanide usually exists in several of forms such as salts and HCN and in the form of complexes[2-6]. Cyanides are weakly bonded within soils, so they often form complexes with other metallic pollutants from effluents, such as Cu, Fe, Zn and Ni and remain in the water. Cyanides complexed by metals are classified in accordance with the strength of the metal cyanide bond. Free cyanides such as cyanide anion and hydrogen cyanide are considered the most toxic forms. Cyanide complexes with cadmium, copper, nickel and zinc are considered as weak-acid dissociable (WAD)[5,6]. Cyanide-complexes with gold, cobalt, silver and iron are considered as strong-acid dissociable (SAD)[5,6]. Cyanides also presents as organic cyanides such as acrylonitrile and propinonitrile[7,8]. Cyanides concentration in the environment mainly depends on the type of human activities. The normal cyanide levels found in unpolluted stream and lake water is in the range between 0.001-0.05 mg/L[9]. Regular industrial effluents contain a range between 0.01 and 10 mg/L of the total measured cyanide[9], meanwhile some other industrial effluents such as that produced from electroplating plants contain higher cyanide levels[9] than 100,000 mg/L. Hence, it is very important that effluents from different industries must be treated before released to the environment to prevent the pollution. Therefore, restrictive concentrations for discharge of cyanide bearing wastewater to sewers were imposed by many countries. For example, the proposed limits for the total cyanide in aquatic-biota waters and drinking regarding are 50 and 200 ppb, respectively, was imposed by the USEPA. Whereas, the limit of 0.01 mg/L for surface water cyanide and 0.5 mg/L for sewers cyanide was imposed by the German and Swiss regulations[10]. Accordingly, cyanide removal, degradation and/or recycle are crucial for reducing the cyanides concentration in different aquatic environments lower than regulatory limits. Adsorption, complexation and oxidation are well known process used for treating cyanides in polluted water[11,12]. Unfortunately, most of these treatment processes are not efficient and produce more toxic and problematic compounds[13]. During the last three decades, photocatalytic oxidation of cyanide in waste water using solar light was explored as alternative process[14]. Several studies showed the applicability for the degradation of cyanide in wastewater. Titanium dioxide is non-toxic catalyst, recyclable,

with high efficiency[15-17]. Photocatalytic degradation of dyes by TiO_2 particles under UV or visible light was the focus of many researchers for its high efficiency compared with conventional treatment processes[16,17]. Titanium dioxide exists in two different crystalline forms *i.e.*, anatase and rutile. Anatase form is the most applicable for environmental remediation due to its exceptional properties; photo-stability under most conditions and water insolubility, in addition to the non-toxicity and low cost[17]. Nevertheless, the application of TiO_2 as a photocatalyst for wastewater treatment *via* photocatalytic oxidation is very limited due to its low photodegradation effectiveness. Many researchers devoted their work to enhance the TiO_2 photodegradation efficiency by doping with other noble metals, but these modifications slightly enhanced the TiO_2 photocatalytic activity or few cases decreased the efficiency. Silver sulfide can be used in photovoltaic cells, IR detectors and photoconductors due to its thermoelectric and photoelectric properties[18-23]. Silver sulfide has narrow band gap energy and chemical stability[24]. Many methods are used to prepare silver sulfide, for example, organic-metallic precursor; γ-irradiation; sonochemical method; template; sol-gel and microemulsions methods[25-30]. In the present study, we studied the improvement of photocatalytic activity of silver sulfide by gold doping, also, effect of wt % of gold was studied.

EXPERIMENTAL

Synthesis of silver sulfide (Ag_2S): Silver sulfide nanoparticles were synthesized by hydrothermal way as the following: Silver chloride (2.5 mmol) and thioacetamide (10 mmol) are dissolved in deionized water (40 mL). The obtained mixture was heated for 24 h at 200 °C in Teflon-lined stainless steel autoclave. The solid materials are collected by filtration and wash many times by deionized water and absolute ethanol. Finally, dried for 3 h and 80 °C under vacuum.

Synthesis of Au/Ag_2S: Photoassisted deposition method was used to prepare Au/Ag_2S with different wt % of gold such as 0.2, 0.4, 0.6 and 0.8 wt % of Au metal. Doping of gold into silver sulphide was carried out as the following: Silver sulfide nanoparticle was dispersed into an aqueous solution of $HAuCl_4$ in presence of UV light irradiation. Finally, the obtained samples were dried for 24 h at 60 ºC, then annealed under hydrogen gas for 2 h at 150 ºC.

Photocatalyst characterization: A Bruker axis D8 was used to measure XRD pattern of the prepared photocatalyst at room temperature. A Nova 2000 series chromatech apparatus was used to determine surface area of the prepared photocatalyst samples. Before determination of the BET, the prepared photocatalysts were heated under vacuum for 2 h at 120 ºC. A UV/visible/NIR spectrophotometer (V-570, JASCO, Japan) was used to determine band gap energy of the prepared photocatalysts. A JEOL-JEM-1230 microscope was used to determine shape and size of the prepared photocatalyst. Before measurements, the prepared photocatalyst was dispersed in ethanol by ultrasonication, then the dispersed photocatalyst sample is located into carbon-coated copper grid. A Thermo Scientific K-ALPHA, XPS, England was used to determine XPS of the prepared photocatalyst. Pl of the prepared photocatalysts was measured by a Shimadzu RF-5301 fluorescence spectrophotometer.

Testing of photocatalytic performance of prepared photocatalyst: Cyanide was chosen to determine photocatalytic performance of the prepared photocatalyst. Testing was carried out in batch reactor. A blue fluorescent lamp which is doubly covered by UV cut filter was used to irradiate photocatalyst. UV radiometer confirm that the intensity of UV light is under limit of detection. A required weight of the photocatalyst was dispersed in potassium cyanide solution (volume 300 mL and concentration 100 ppm) and pH of the mixture was adjusted at 10.5 to a void HCN gas evolution by ammonia solution. A volumetric titration with $AgNO_3$ was used to measure CN ion concentration by potassium iodide. Photocatalytic degradation efficiency, % was calculated by the following equation:

$$\% \text{ Photocatalytic degradation efficiency} = (Co - C)/C_o \times 100$$

where C_o is initial concentration of cyanide and C is concentration of cyanide at time t.

RESULTS AND DISCUSSION

Photocatalyst characterization: Fig. 1. shows XRD patterns of Ag_2S and Au/Ag_2S nanoparticles. The results reveal that XRD patterns of all prepared samples is composed of Ag_2S. There is no diffraction peak for gold or gold oxide. This indicate that gold may be well dispersed into Ag_2S nanoparticles. Also, results reveal that increase wt % of gold decrease intensity of Ag_2S peaks. Scherer's equation was used to calculate

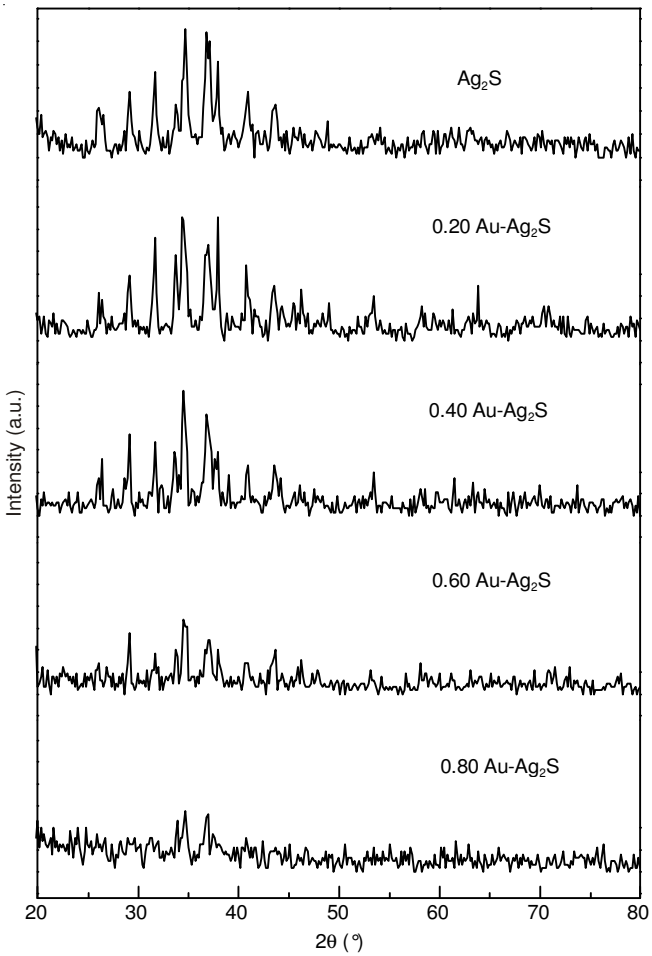

Fig. 1. XRD pattern of Ag_2S and Au/Ag_2S nanoparticles

0 crystallite sizes of Ag_2S. The crystallite size of the Ag_2S, 0.2 wt % Au/Ag_2S, 0.4 wt % Au/Ag_2S, 0.6 wt % Au/Ag2S and 0.8 wt % Au/Ag_2S were 24, 19, 16, 13 and 10 nm, respectively. As wt % of gold increased the crystallite size of Ag_2S became smaller.

Fig. 2. shows XPS spectres of 0.6 wt % Au/Ag_2S nanoparticles. The results reveal that silver species are existed as +1 oxidation state as shown in Fig. 2a and sulfur species are existed -2 oxidation state as shown in Fig. 2b, which appears at binding energy of 367.8, 374 eV and 160.9, 161.9 eV for Ag $_3$d and S_2p, respectively. Gold species are existed as metal gold as shown in Fig. 2c, which appears at binding energy of 87.7 eV and 84.0 eV.

Fig. 3. shows TEM images of Au/Ag_2S nanoparticles. The results reveal particle size of gold increased as wt % of gold increased. Dispersion of gold increased as wt % of gold increased. Also, As wt % of Au increased from 0 to 0.6 wt % the homogeneity of Au above Ag_2S increased, but homogeneity of Au decreased at high wt % of Au over 0.6 wt %. Therefore, 0.6 wt % Au is the optimum wt %.

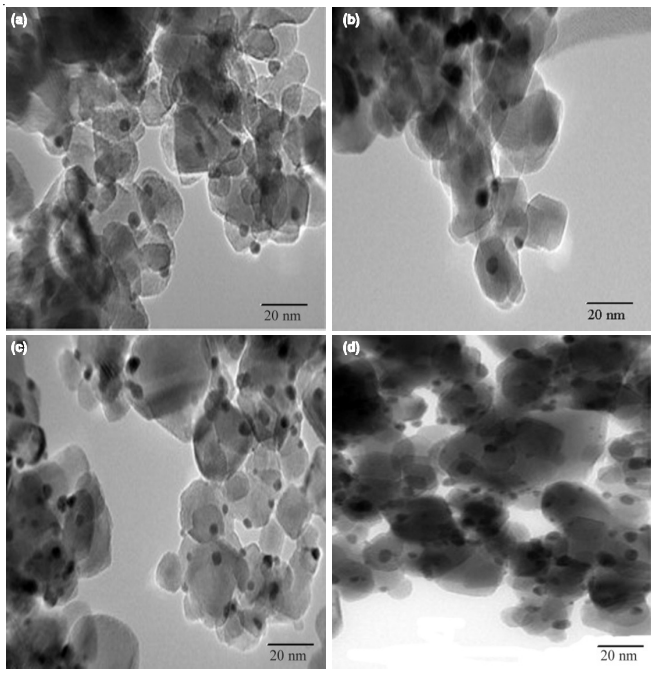

Fig. 3. TEM images of Au/Ag_2S nanoparticles, where wt % of Au is 0.2 (a), 0.4 (b), 0.6 (c) and 0.8 (d)

Surface area measurement: Surface area of Ag_2S and Au/Ag_2S nanoparticles were determined. The S_{BET} values were 50, 48, 45, 43 and 41 m^2/g for the Ag_2S, 0.2 wt % Au/Ag_2S, 0.4 wt % Au/Ag_2S, 0.6 wt % Au/Ag_2S and 0.8 wt % Au/Ag_2S, respectively. Table-1 shows that surface area parameters of Ag_2S and Au/Ag_2S nanoparticles. Au/Ag_2S nanoparticles have total pore volume smaller than that of Ag_2S nanoparticles. Because deposition of gold block some pore of Ag_2S nanoparticles.

Optical characterization: Fig. 4. shows UV-visible spectra of Ag_2S and Au/Ag_2S nanoparticles. The results reveal that increase wt % of gold from 0.2 to 0.8 wt % increase absorption edge from 396 to 453 nm, respectively, in compare to 376 nm absorption edge of Ag_2S. Table-2 shows band gap energy of Ag_2S and Au/Ag_2S nanoparticles, which calculated from UV-visible spectra. The band gap energy are 3.30, 3.13, 2.86, 2.76 and 2.74 eV for the Ag_2S, 0.2 wt % Au/Ag_2S, 0.4 wt % Au/Ag_2S, 0.6 wt % Au/Ag_2S and 0.8 wt % Au/Ag_2S, respectively. Fig. 5. shows Pl spectra Ag_2S and Au/Ag_2S nanoparticles. The results reveal that increase wt % of gold decrease pl peak intensity. Therefore, Au can separate electron and hole pairs and increase photocatalytic activity.

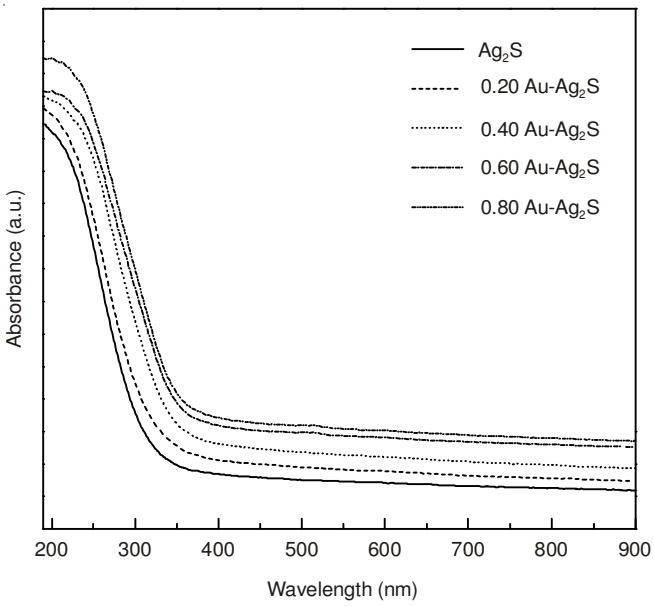

Fig. 4. UV-visible absorption spectra of Ag_2S and Au/Ag_2S nanoparticles

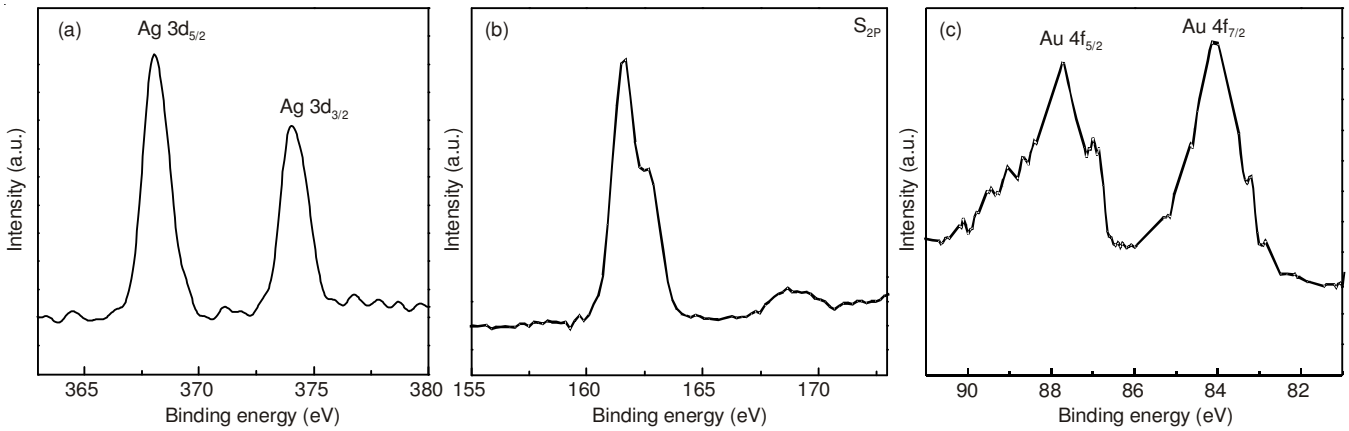

Fig. 2. XPS spectres for 0.60 Au/ Ag2S, where (a) for Ag 3d ; (b) for S 2p and (c) for Au 4f

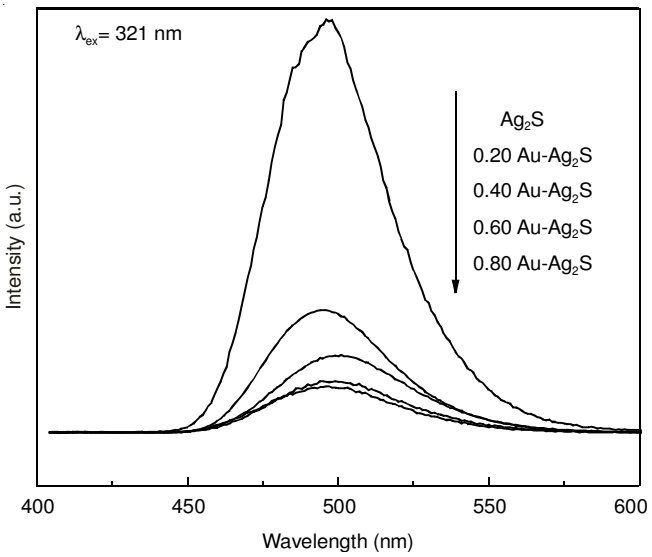

Fig. 5. Photoluminescence spectra of Ag_2S and Au/Ag_2S nanoparticles

TABLE-1
TEXTURE PARAMETERS OF
Ag_2S AND Au-Ag_2S NANOPARTICLES

Sample	S_{BET}(m^2/g)	S_t(m^2/g)	Total V_P(mL/g)	r(Å)
Ag_2S	50.00	53.00	0.180	44.00
0.20 Au/Ag_2S	48.00	49.00	0.174	46.00
0.40 Au/Ag_2S	45.00	47.00	0.171	49.00
0.60 Au/Ag_2S	43.00	45.00	0.168	53.00
0.80 Au/Ag_2S	41.00	43.00	0.164	62.00

S_{BET}: BET surface area; S_t: Surface area derived from V_{l-t} plots: r⁻: mean pore radius V_p: Total pore volume

TABLE-2
BAND GAP ENERGY OF Ag_2S AND Au/Ag_2S NANOPARTICLES

Sample	Band gap energy (eV)
Ag_2S	3.30
0.20 Au/Ag_2S	3.13
0.40 Au/Ag_2S	2.86
0.60 Au/Ag_2S	2.76
0.80 Au/Ag_2S	2.74

Testing of the photocatalytic performance: In general, the process for photocatalysis begins when photons transfer from conduction band to valance band, which produce electron and hole pairs. This is followed by diffusion of the charge carriers to the surface of the particle where the interaction with water molecules would produce highly reactive species of peroxide (O_2^-) and hydroxyl radical ($OH^\bullet$) responsible for the degradation of adsorbed organic molecules. Step-reactions in the photocatalytic process leading to the degradation of CN^- are presented in the following sequence:

$$Ag_2S + h\nu \rightarrow e^- + h^+$$

$$e^- (Au) \rightarrow e_{tr}^- (Au)$$

$$e_{tr}^- + O_2 (ads) \rightarrow O_2^-$$

$$2\ e_{tr}^- + 2H^+ + O_2 \rightarrow H_2O_2$$

$$H_2O_2 + e_{tr}^- \rightarrow OH^- + OH^\bullet$$

$$h^+ + H_2O \rightarrow H^+ + OH^\bullet$$

$$2CN^- + 4\ OH^\bullet \rightarrow 2N_2 + 2CO_2 + 2H_2$$

The photocatalytic degradation of cyanide by Ag_2S and Au/Ag_2S nanoparticles is shown in Fig. 6. The results reveal that photocatalytic degradation of cyanide, % are 14 and 16 % for Ag_2S and 0.20 wt % Au/Ag_2S, respectively. Because, the reaction was carried out under visible light irradiation and Ag_2S and 0.20 wt % Au/Ag_2S absorb in UV region. Also, photocatalytic degradation of cyanide, % increased as wt % of Au increased. 0.60 wt % Au/Ag_2S has highest photocatalytic activity, % (99 % after 60 min).

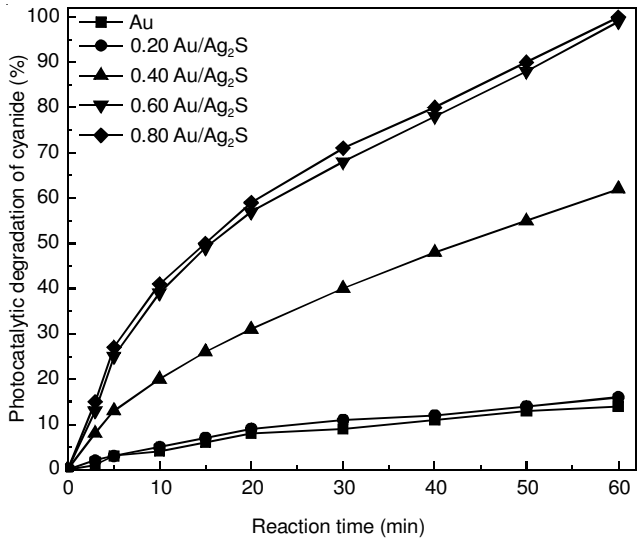

Fig. 6. Effect of the catalyst type on the photocatalytic oxidation of cyanide

Fig. 7. shows effect of weight of photocatalyst on photocatalytic degradation of cyanide, %. The results reveal that photocatalytic degradation of cyanide, % increased from 63 to 99 % after 60 min by increase weight of photocatalyst increase from 0.1 to 0.3 g, respectively. Reaction time which required for complete degradation of cyanide decreased from 60 to 40 min by increase weight of photocatalyst from 0.3 to 0.4 g. Reaction time which required for complete degradation of cyanide increased again by increase weight of photocatalyst above 0.4 g, due to excessive weight of photocatalyst block light penetration.

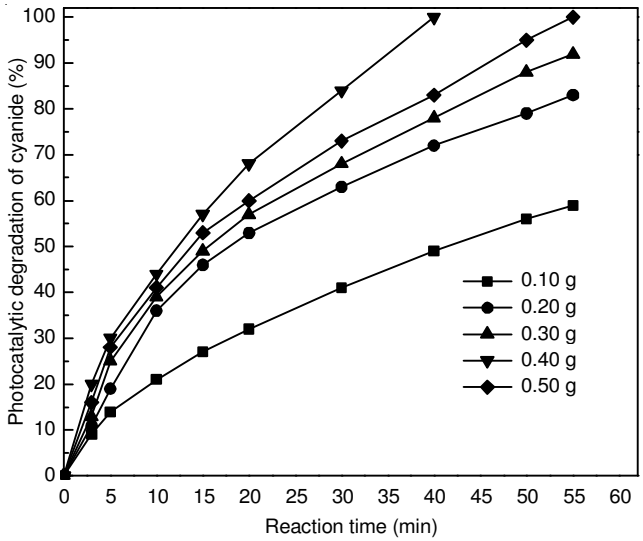

Fig. 7. Effect of the loading of 0.60 Au/Ag_2S on the photocatalytic oxidation of cyanide

Photocatalyst recycling: 0.60 wt % Au/Ag_2S was used for five times and the results are shown in Fig. 8. The results reveal that photocatalytic degradation of cyanide, % , remain unchanged after used five times. Therefore, 0.60 wt % Au/Ag_2S photocatalyst is stable and shows potential for green remediation applications.

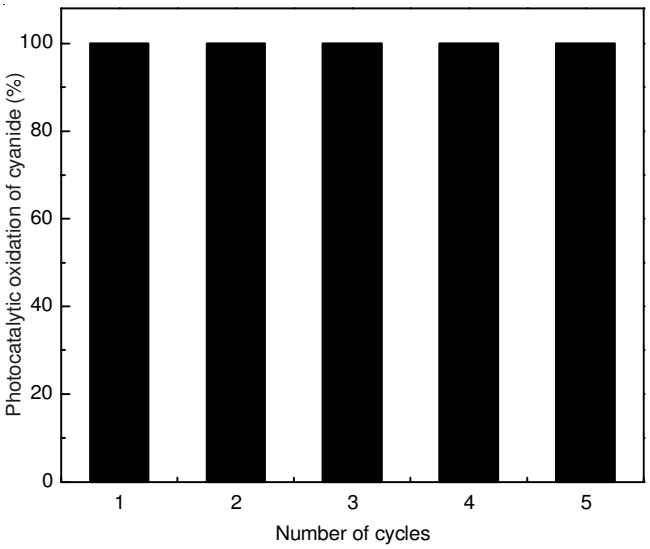

Fig. 8. Reuse of photocatalysts in the photocatalytic oxidation of cyanide

Conclusion

Hydrothermal method was used to prepare Ag_2S nanoparticles, photoassisted deposition method (PAD) was used to doped gold into Ag_2S nanoparticles. Doping of Au decease band gap energy of Ag_2S to visible light region. 0.60 wt % Au/Ag_2S photocatalyst has the highest photocatalytic activity at weight 0.4 g; volume of KCN solution 300 mL; KCN concentration 100 ppm; reaction time 40 min. Photocatalytic activity of 0.60 wt % Au/Ag_2S photocatalyst is stable after reuse five times.

REFERENCES

1. D. Park, D.S. Lee, Y.M. Kim and J.M. Park, *Bioresour. Technol*., **99**, 2092 (2008).
2. F. Gurbuz, H. Ciftci and A. Akcil, *J. Hazard. Mater*., **162**, 74 (2009).
3. A. Chergui, R. Kerbachi and G. Junter, *Chem. Eng. J*., **147**, 150 (2009).
4. A. Akcil, *Biotechnol. Adv*., **21**, 501 (2003).
5. M.M. Botz, Overview of Cyanide Treatment Methods, Mining Environmental Management, Mining Journal Ltd., London, UK, pp. 28-30 (2001).
6. S. Ebbs, *Curr. Opin. Biotechnol*., **15**, 231 (2004).
7. C.M. Kao, K.F. Chen, J.K. Liu, S.M. Chou and S.C. Chen, *Appl. Microbiol. Biotechnol*., **71**, 228 (2006).
8. R.R. Dash, A. Gaur and C. Balomajumder, *J. Hazard. Mater*., **163**, 1 (2009).
9. R.R. Dash, C. Balomajumder and A. Kumar, *Iran. J. Environ. Health Sci. Eng*., **3**, 91 (2006).
10. J. Shen, H. Zhao, H. Cao, Y. Zhang and Y. Chen, *J. Environ. Sci. (China)*, **26**, 231 (2014).
11. A. Valiuniene, G. Baltrunas, V. Keršulyte, •. Margarian and G. Valincius, *Process Saf. Environ. Prot*., **91**, 269 (2013).
12. M. Hijosa-Valsero, R. Molina, H. Schikora, M. Müller and J.M. Bayona, *Water Res*., **47**, 1701 (2013).
13. G.J. Zagury, K. Oudjehani and L. Deschenes, *Sci. Total Environ*., **320**, 211 (2004).
14. R.M. Mohamed and E.S. Baeissa, *Appl. Catal. A*, **464-465**, 218 (2013).
15. H. Liu, A. Imanishi and Y. Nakato, *J. Phys. Chem. C*, **111**, 8603 (2007).
16. M.R. Hoffmann, S.T. Martin, W. Choi and D.W. Bahnemann, *Chem. Rev*., **95**, 69 (1995).
17. Y. Yu, J.C. Yu, C.-Y. Chan, Y.-K. Che, J.-C. Zhao, L. Ding, W.-K. Ge and P.-K. Wong, *Appl. Catal. B*, **61**, 1 (2005).
18. T. Ben Nasr, H. Maghraoui-Meherzi, H. Ben Abdallah and R. Bennaceur, *Solid State Sci*., **26**, 65 (2013).
19. H. Shen, X. Jiao, D. Oron, J. Li and H. Lin, *J. Power Sources*, **240**, 8 (2013).
20. S. Xu, G. Liu, J. Li and G. Qiao, *Mater. Lett*., **64**, 347 (2010).
21. Y. Sun, B. Zhou, P. Gao, H. Mu and L. Chu, *J. Alloys Comp*., **490**, L48 (2010).
22. S. Hull, D.A. Keen, D.S. Sivia, P.A. Madden and M. Wilson, *J. Phys. Condens. Matter*, **14**, 9 (2002).
23. T. Minami, *J. Non-Cryst. Solids*, **95-96**, 107 (1987).
24. Y.P. Sun, J.E. Riggs, H.W. Rollins and R. Guduru, *J. Phys. Chem. B*, **103**, 77 (1999).
25. J.C. Liu, P. Raveendran, Z. Shervani and Y. Ikushima, *Chem. Commun.*, 2582 (2004).
26. L. Armelao, R. Bertoncello, E. Cattaruzza, S. Gialanella, S. Gross, G. Mattei, P. Mazzoldi and E. Tondello, *J. Mater. Chem*., **12**, 2401 (2002).
27. J.P. Xiao, Y. Xie, R. Tang and W. Luo, *J. Mater. Chem*., **12**, 1148 (2002).
28. R.V. Kumar, O. Palchik, Y. Koltypin, Y. Diamant and A. Gedanken, *Ultrason. Sonochem*., **9**, 65 (2002).
29. M. Chen, Y. Xie, H.Y. Chen, Z.P. Qiao and Y.T. Qian, *J. Colloid Interf. Sci*., **237**, 47 (2001).
30. W.P. Lim, Z. Zhang, H.Y. Low and W.S. Chin, *Angew. Chem. Int. Ed*., **43**, 5685 (2004).